

# First Results from the CHEPS\*: Exoplanets and the Discovery of an Eccentric Brown Dwarf in the Desert†

J.S. Jenkins<sup>1</sup>, H.R.A. Jones<sup>2</sup>, K. Goździewski<sup>3</sup>, C. Migaszewski<sup>3</sup>, J.R. Barnes<sup>2</sup>,

M.I. Jones<sup>1</sup>, P. Rojo<sup>1</sup>, D.J. Pinfield<sup>2</sup>, A.C. Day-Jones<sup>2</sup>, S. Hoyer<sup>1</sup>

<sup>1</sup>*Department of Astronomy, Universidad de Chile, Casilla 36-D, Santiago, Chile, email: jjenkins@das.uchile.cl*

<sup>2</sup>*Center for Astrophysics, University of Hertfordshire, College Lane Campus, Hatfield, Hertfordshire, UK, AL10 9AB*

<sup>3</sup>*Toruń Centre for Astronomy, Nicolaus Copernicus University, Gagarina 11, 87-100 Toruń, Poland*

Draft: 11/08

## ABSTRACT

We report the discovery of a brown dwarf on an eccentric orbit and with a semimajor axis that places it in the brown dwarf desert region around the star HD191760. The star has a spectral type of G3IV/V and a metallicity ( $[\text{Fe}/\text{H}]$ ) of 0.29 dex. HD191760 adds to the small number of metal-rich stars with brown dwarf companions. The brown dwarf (HD191760*b*) is found to have an orbital period of  $505.57 \pm 0.40$  days and semimajor axis of  $1.35 \pm 0.01$  AU, placing it firmly in the brown dwarf desert. The eccentricity of HD191760*b* is found to be  $0.63 \pm 0.01$ , meaning it reaches as close as 0.5 AU from the host star. Dynamical simulations indicate that no inner planets could reside at separations beyond  $\sim 0.17$  AU due to the disastrous gravity imposed by HD191760*b*. In addition to these first results we also refine the orbits found for the exoplanets around the stars HD48265, HD143361 and HD154672. All 1-planet solutions are in agreement with those previously published by the Magellan Planet Search.

## Key words:

stars: low-mass, brown dwarfs – planetary systems – techniques: radial velocities

## 1 INTRODUCTION

Since the first few extrasolar planets (hereafter exoplanets) were detected (Mayor & Queloz 1995; Marcy & Butler 1996a; Marcy & Butler 1996b) it became readily apparent that planets preferred metal-rich environments (Gonzalez 1997). This discovery has been placed in the framework of giant planet formation through core accretion of gas depleted materials left over from the formation of the parent star (e.g. Kornet et al. 2005; Alibert et al. 2005). This hypothesis has been extensively tested by different methods and analysis techniques, most recently by Fischer & Valenti (2005), and remains the most plausible scenario for the increased probability of planet detection around metal-rich stars. The competing theory is based on the concept that planets migrate through the proto-planetary disks from which they formed (Lin & Papaloizou 1986; Trilling et al. 2002). It has been hy-

pothesized that the stellar atmosphere is polluted after formation through infall of migrating planets onto the stellar surface. However, Pinsonneault et al. (2001) modelled the infall of material onto stellar atmospheres at the ZAMS and found that  $10 M_{\oplus}$  worth of gas depleted material could raise the metallicities ( $[\text{Fe}/\text{H}]$ ) of G dwarfs to  $\sim 0.3$  dex, whereas the same material falling on an F dwarf would increase the metallicity to  $\sim 0.6$  dex. In their large sample ( $>1000$  stars) of consistent metallicities, Fischer & Valenti found no correlation between the depth of convective zones of exoplanet hosts and their metallicity, indicating that infall of planets or gas depleted material can not explain the over abundance of metal-rich atmospheres for exoplanet host stars.

Whatever the scenario that leads to exoplanet host stars being rich in metals, it is clear that such stars have a higher probability of hosting exoplanets. Fischer & Valenti have determined that the fraction of planets increases with increasing metallicity proportional to the square of the number of iron atoms in the stellar photosphere. This correlation is being exploited by a number of planet search projects like the N2k, Keck, etc who bias their samples, or subsets thereof, towards the most metal-rich stars. We are exploiting this

\* Calan-Hertfordshire Extrasolar Planet Search

† Based on observations collected at the La Silla Paranal Observatory, ESO (Chile) with the HARPS spectrograph on the ESO 3.6m telescope, under the program IDs 079.C-0927(B), 079.C-0927(C), 081.C-0148(A), 081.C-0148(B) and 282.C-5034.

correlation also, by searching around the most metal-rich solar-type stars in the southern hemisphere as part of our CHEPS project. The CHEPS target list is compiled from the analysis of Jenkins et al. (2008) by utilising high S/N high resolution spectra, acquired using the FEROS spectrograph (Kaufer et al. 1999). The targets were selected to have  $[\text{Fe}/\text{H}] \geq 0.1$  dex and all have  $B - V$  colours in the range 0.5–0.9 (Spectral Types of late-F to mid-K). Along with the metallicity bias we are also focusing on the most inactive stars. The Ca II HK line cores were used in Jenkins et al. to measure the  $\log R'_{\text{HK}}$  activity index (Noyes et al. 1984) which has been shown to be a useful proxy to the level of noise (aka *jitter*) in radial-velocity timeseries (Saar & Donahue 1997; Saar et al. 1998; Wright 2005). We therefore selected our primary sample to include all stars with  $\log R'_{\text{HK}} \leq -4.5$ , which allows for the lowest levels of radial-velocity jitter in our dataset.

## 2 OBSERVATIONS

We present data from six observing runs using the ESO-HARPS instrument (Mayor et al. 2003) on the 3.6m telescope in La Silla Chile. HARPS is a fiber-fed cross-dispersed echelle spectrograph. The instrument employs two 1" on sky fibers, one on object and one on the Thorium-Argon (ThAr) calibration source, which feed the light to the spectrograph to be re-imaged on two 2k4 CCD chips. A total of 72 orders are spread over the two CCD's, 36 object and 36 calibration source, with an instrumental resolution ( $R$ ) of  $\sim 115,000$ . 29 observations were made of HD191760, with 8 for HD48265 and 6 each for both HD143361 and HD154672, all using our standard observational procedure, which aims to observe each star for a fixed integration time of 15 minutes in order to integrate over the strongest p-mode oscillations that all solar-like stars exhibit (O'Toole et al. 2008). Also to attempt to increase our efficiency to the detection of short period exoplanets, and in particular low mass exoplanets, we intensively monitor the stars on short timescales to search for potential planetary signals, including for HD191760.

The reduction and analysis of all stars are performed in near real time at the telescope, using the latest version of the HARPS-DRS (Pepe et al. 2004). The DRS (Data Reduction Software) performs all functions of the reduction and analysis, from bias removal, order localisation, flatfielding, cosmic ray removal, scattered light subtraction, extraction and blaze correction, to determination of the radial-velocities, barycentric Julian dates and internal uncertainties through cross-correlation with stellar templates and the reference ThAr calibration orders. Due to the high quality mechanical, thermal and pressure stabilisation of HARPS, the drift over a single night is found to be less than 1 m/s. Such a system provides internal uncertainties below 1 m/s, meaning our short term precision is dominated by stellar activity induced jitter (e.g. Saar et al. 1998).

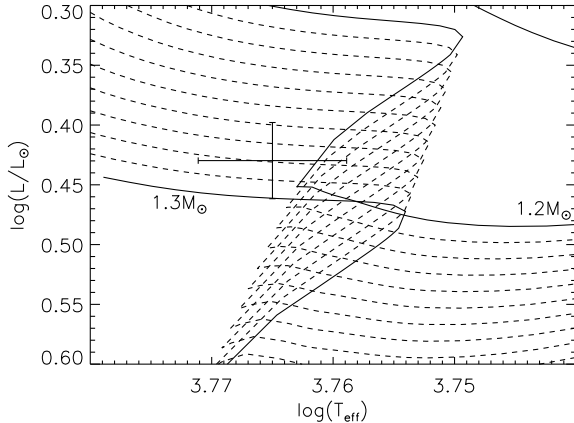
## 3 HD191760 CHARACTERISTICS

Table 1 lists the stellar characteristics of the star HD191760. Houk (1978) lists the star's spectral type as G3IV/V, which is in agreement with the value adopted by Hipparcos

(Perryman et al. 1997; van Leeuwen 2007) and also with the derived distance from the Hipparcos main sequence ( $\Delta M_V$ ; Jenkins et al. 2008). All Hipparcos astrometry was obtained using the AstroGrid tool which lists the new catalogue values from van Leeuwen with increased astrometric precision. The kinematic catalogue of Nordström et al. (2004), later updated by Holmberg et al. (2007), includes observations of HD191760 through Strömgren filters and calibrations based on the infrared flux method (Alonso et al. 1996) to derive various stellar characteristics. They also used parallax measurements from Hipparcos, along with Padova evolutionary tracks (Girardi et al. 2000) to determine evolutionary parameters for their sample. We have also derived various parameters for a number of stars in preparation for our metallicity based planet search, both by high resolution FEROS spectra and precise photometry. We used the Hipparcos optical magnitudes, along with 2MASS photometry, to measure the effective temperatures of our stars by the infrared flux method (Blackwell et al. 1990). We used these temperatures to interpolate a grid of high resolution Kurucz model atmospheres (Kurucz 1993), built using WITA6 (Pavlenko 2000), to determine the stellar metallicity. Yonsei-Yale (Y2) isochrones (Demarque et al. 2004) were then interpolated using these temperatures, metallicities and an estimate for the alpha-enhancement parameter that was obtained by the locus of points in Edvardsson et al. (1993) and Pagel & Tautvaisiene (1995).

The properties of HD191760 derived by Holmberg et al. and this work mostly agree within the formal uncertainties. Their metallicity value of  $0.12 \pm 0.10$  dex is found to be smaller than our value of  $0.29 \pm 0.07$  dex and Holmberg et al. (2008) show that there is a small systematic offset between their metallicities and those published in Jenkins et al. due to the differing effective temperature scales employed. Fig. 1 shows the position of HD191760 on an HR-diagram, along with the Y2 isochrones in steps of  $0.1 M_{\odot}$  (solid curves) and higher resolution steps of  $0.01 M_{\odot}$  (dashed curves). The position of the star, given the bolometric luminosity of  $2.69 \pm 0.2 L_{\odot}$ , effective temperature of  $5821 \pm 82 \text{K}$  and  $[\text{Fe}/\text{H}]$  of  $0.29 \pm 0.07$  dex, is best explained by a star of mass  $1.28_{-0.10}^{+0.02} M_{\odot}$ , where the uncertainties are dominated by the uncertainty on the Hipparcos parallax. Our estimate for the age of the star is  $4.1_{-2.8}^{+0.8} \text{Gyrs}$ . The large lower error bars arise due to the position of the star close to the main sequence turnoff. The surface gravity ( $\log g$ ) value of  $4.13_{-0.04}^{+0.05}$  dex is consistent with a star evolving onto the sub-giant branch.

As part of the analysis we performed to select our target sample we also extracted chromospheric activity indices from measurements of the level of emission in the Ca II HK lines. The  $\log R'_{\text{HK}}$ -index has been shown to correlate well with the level of noise (aka jitter) in precise radial-velocity datasets (e.g. Santos et al. 2000; Wright 2005). Fig. 2 shows the Ca II H line core of HD191760 (top) along with the other three planet-host stars we present data for in §5. Our low derived value of  $\log R'_{\text{HK}} = -5.17$  is highlighted from the deep central line core, or lack of core re-emission, of HD191760.



**Figure 1.** Evolutionary Y2 mass tracks are shown in steps of  $0.1M_{\odot}$  (solid curves) and finer steps of  $0.01M_{\odot}$  (dashed curves) for effective temperatures and bolometric luminosities. HD191760 is represented by the error bars and its position is consistent with a mass of  $1.28^{+0.02}_{-0.10}M_{\odot}$  and an age of  $4.21^{+0.5}_{-2.8}$  Gyrs. The masses of the solid curves are shown for reference.

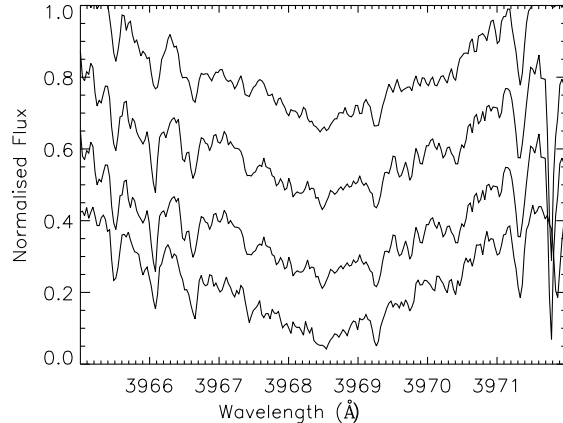


**Figure 2.** The calcium II H line cores for the four stars discussed in this work. From top to bottom we show HD191760, HD48265, HD143361 and HD154672 respectively. All four objects exhibit no re-emission of flux in the line core, highlighting the inactive nature of these stars.

**Table 1.** Stellar parameters for HD191760.

Parameter	HD191760
Spectral Type	G3IV/V
$\log R'_{\text{HK}}$	-5.17
Hipparcos $N_{\text{obs}}$	99
Hipparcos $\sigma$	0.011
$\pi$ (mas)	$12.25 \pm 0.90$
$\Delta M_V$	1.107
$L_*/L_{\odot}$	$2.69 \pm 0.20$
$M_*/M_{\odot}$ - H07	$1.14^{+0.08}_{-0.05}$
$M_*/M_{\odot}$ - Here	$1.28^{+0.02}_{-0.10}$
$R_*/R_{\odot}$	$1.62 \pm 0.07$
$T_{\text{eff}}$ (K) - H07	$5794 \pm 76$
$T_{\text{eff}}$ (K) - J08	$5821 \pm 82$
[Fe/H] - H07	$0.12 \pm 0.10$
[Fe/H] - J08	$0.29 \pm 0.07$
$\log(g)$	$4.13^{+0.05}_{-0.04}$
U, V, W - H07 (km/s)	-29, -21, 15
$v \sin i_{R'_{\text{HK}}}$ (km/s)	3.47
$v \sin i_{\text{H07}}$ (km/s)	2
$v \sin i_{\text{CCF}}$ (km/s)	$2.33 \pm 0.05$
$P_{\text{rot}, R'_{\text{HK}}}$ (days)	25.2
$P_{\text{rot}, \text{CCF}}$ (days)	35.1
$\text{Age}_{R'_{\text{HK}}}$ (Gyrs)	9.9
Age (Gyrs) - H07	$5.6^{+0.9}_{-1.9}$
Age (Gyrs) - Here	$4.1^{+0.8}_{-2.8}$
Jitter - $\log R'_{\text{HK}}$ (m/s)	1.50

H07 relates to Holmberg et al. (2007), J08 is the reference for Jenkins et al. (2008) and Here labels values derived in this work.

#### 4 ORBITAL SOLUTION FOR HD191760

The 29 Doppler velocities for HD191760 were measured in six observing runs, four of which spanned five nights in duration, with the final two points acquired through ESO Directors Discretionary Time. All velocities and bisector span values (BVS) are listed in Table 2, note that the two large deviant BVS values are from our two lowest quality spectra which were interrupted by clouds, significantly lowering

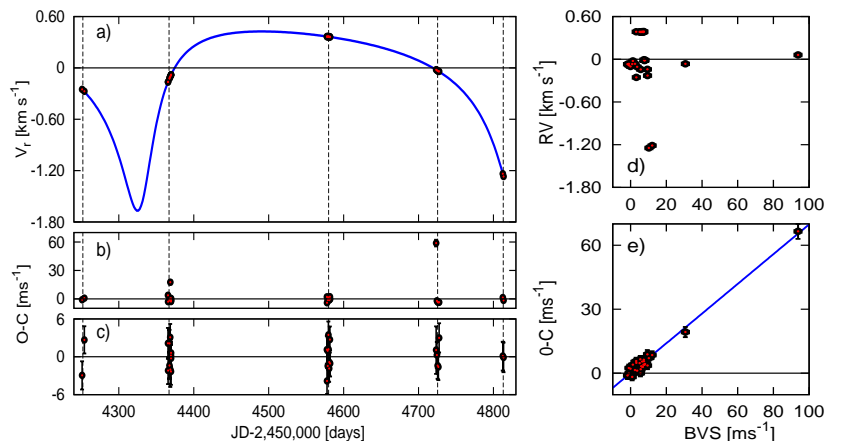


**Figure 3.** Panel (a) shows the best fit Keplerian solution to the Doppler points for HD191760 with BVS correction as in Migaszewski & Nowak (2009). The data come from six observing runs spread over a full orbital period of the companion. The addition of two Doppler points close to periastron passage was used to confirm the eccentric nature of the companion. Panel (b) shows the residuals without BVS correction and panel (c) shows the residuals after correction, corresponding to the synthetic curve in panel (a). Panel (d) shows the radial-velocities against the BVS after subtraction of the best fit Keplerian synthetic curve. Panel (e) shows the best fit linear correlation coefficient of BVS-RV. Note that the two values with the largest BVS help to better constrain the correlation.

the S/N, meaning the construction of the CCF was much poorer than the rest of the high S/N spectra acquired. Panel (a) in Fig. 3 shows these velocities with the best fit Keplerian solution to the data. Due to the scheduling of the runs the orbit is firmly constrained by the final two data points. Before the final two data points were acquired, a resonant double planet solution could describe the dataset just as well. Such system ambiguities could be common in radial-velocity datasets, particularly at low eccentricities (Anglada-Escude et al. 2008). However, in this case the system configurations were so contrasting that one data point was enough to decouple them, and with an eccentricity of around 0.63 and no indication of any trend in the third ob-

**Table 2.** Radial-velocities for HD191760

BJD (-2454000)	RV (m/s)	Uncertainty (m/s)	BVS (m/s)	RV- $\alpha$ BVS (m/s)
250.90047	-30662.99	0.88	9.49	-235.23
253.89490	-30689.15	0.70	3.20	-257.01
365.50781	-30575.97	1.37	9.45	-148.19
365.73781	-30577.79	0.62	5.68	-147.39
367.49679	-30540.86	0.38	3.66	-109.04
367.72155	-30535.38	0.73	-0.09	-100.95
368.49981	-30519.40	0.53	-0.94	-84.39
368.71411	-30498.29	1.86	30.70	-85.31
369.49468	-30503.67	0.77	-1.71	-68.12
369.62706	-30501.89	0.50	0.91	-68.16
369.68010	-30497.67	0.51	2.50	-65.07
369.74838	-30497.94	0.63	-0.93	-62.93
577.77658	-30045.01	0.82	7.41	384.19
577.90446	-30051.42	0.40	5.55	379.07
578.77151	-30047.07	0.54	6.49	382.77
578.90713	-30049.68	0.48	6.46	380.18
579.74685	-30048.12	0.56	3.12	384.07
579.90348	-30049.27	0.41	5.07	381.57
580.74769	-30052.14	0.60	6.86	377.44
580.89930	-30051.97	0.51	5.94	378.25
581.76210	-30049.85	0.39	5.45	380.71
581.91331	-30052.58	0.36	7.26	376.73
723.53335	-30373.95	3.17	93.78	-4.90
724.55839	-30440.36	0.34	7.46	-11.19
725.53823	-30446.88	0.44	8.10	-18.15
726.53101	-30452.77	0.43	7.76	-23.81
727.53134	-30458.24	1.09	1.25	-24.74
812.52135	-31646.47	1.02	12.07	-1220.52
813.53608	-31679.70	1.16	10.27	-1252.50

servational dataset, which is where a resonant system should most manifest a trend, we believe the quoted solution is accurate. Panel (b) shows the residuals to this fit without correcting for the bisector variations. Such variations have been shown to be a robust tracer of line asymmetries that can impact stellar radial-velocity measurements (Queloz et al. 2001; Henry et al. 2002). We perform corrections for such variations following the analysis in Migaszewski & Nowak (2009) and the residuals for the data after BVS correction is shown in panel (c). The radial-velocities (RV) are shown against the bisector velocity span (BVS) values in panel (d). This highlights the difference of the two offset velocities, particularly one data point which has a BVS value greater than 90m/s. The correlation coefficient ( $\alpha$ ) used to correct the radial-velocities is shown in panel (e) by the solid line. It is clear that the two velocities with large BVS values help to constrain the correlation across the parameter space and indicate the technique is robust, even for fairly large BVS offsets. The  $\alpha$  correction factor is found to be  $0.697 \pm 0.064$  and the corrected radial-velocities, those that are plotted in panel (a), are listed in column 5 of Table. 2. Clearly the data describes the fit much more accurately after BVS correction has been performed, compared with no corrections shown in panel (b). Given the level of the residuals, with uncertainties which include in quadrature the stellar jitter of 1.50 m/s, being all around  $\pm 1\sigma$  from the fit, the quoted orbital solution is accurately constrained. The orbital characteristics for a single companion solution is shown in column 2 of Table. 4.

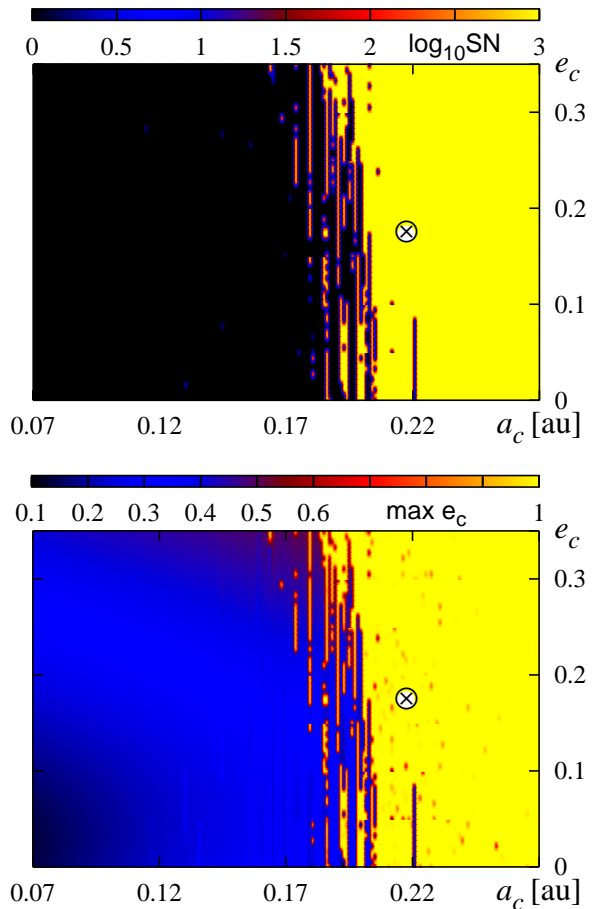


**Figure 4.** Stability maps for a potential planet in semi-major axis–eccentricity space in the HD191760 system. A possible 2-planet solution of reasonable quality and low eccentricity of the inner companion was found, and is shown by the cross. The top panel is for the Spectral Number indicator (Michtchenko & Ferraz-Mello 2001), the lower panel is for the maximal eccentricity attained by the putative planet during  $10^5$  yrs of integration time. The scale at the top of the panels represents the zones of stability, with the darkest regions the most stable. Both indicators around the possible planetary object show no zones of stability anywhere. A sharp border of stable motions is visible. Any planetary companion is unlikely to exist beyond 0.17–0.18 AU regardless of its initial eccentricity.

## 5 POTENTIAL FOR FURTHER COMPANION OBJECTS

In order to map out a strategy for future radial-velocity observations of this star, or indeed to decide if further study is warranted, we decided to look for additional hidden companions in the data. This seems plausible given that the signal describes a fairly wide orbiting companion near the planetary mass boundary, therefore it is reasonable to assume there are other companions in the system with significantly lower mass that would induce a secondary orbital signature with a lower amplitude. Therefore we performed a search for additional companion planets in the system even though the current dataset is rather limited.

First, we tested a hypothesis that the radial-velocity signal may be produced by an additional planet with an intermediate period orbit. We performed the search for additional planets using the genetic algorithm with MEGNO penalty

(GAMP) (Goździewski et al. 2003; Goździewski & Konacki 2006). Essentially, this numerical approach searches the phase space using a genetic algorithm to find zones of stability where additional companions could reside. Unfortunately, the quite extensive GAMP search did not bring any reasonable stable solutions beyond  $\sim 0.2$  AU limit. Actually, we might expect that relatively far from the star, only strongly resonant configurations could be found due to strong gravitational influence of the brown dwarf. We tested this by computing dynamical stability maps for reasonable fits found *without* considering any stability checks. Such an example configuration returns a secondary planetary object with a minimum mass of  $0.10 M_J$ , a low eccentricity of  $\sim 0.17$  and a semimajor axis of  $\sim 0.22$  AU. Such a configuration gives rise to a reduced rms of  $1.84$  m/s and could be hidden in the current dataset. However, as shown in Fig. 4 the entire region around the hypothetical planet is extremely chaotic and therefore it is extremely unlikely that such a planet could reside at this location. The two panels of this figure represent stability maps in the semimajor axis-eccentricity plane in terms of the so called Spectral Number indicator of formally chaotic motions (Michtchenko & Ferraz-Mello 2001, top panel) and the maximum eccentricity indicator (the right-hand panel), i.e. the maximum eccentricity attained during the integration period indicating the degree of geometric instability (large max  $e_c$  means collisions). Both maps were computed over  $10^5$  years that corresponds to  $\sim 50,000$  revolutions of the outer companion. The figure shows that we must rule out, not only this potential companion, but also all companions in the vicinity of this parameter space. Actually, the strongly unstable zone ends at  $\sim 0.17$ – $0.18$  AU, and it is unlikely any other planet could survive the disastrous, short-term perturbations of the brown dwarf companion beyond that limit.

## 6 DISCUSSION

### 6.1 Brown Dwarf Companion

The constrained orbital parameters for HD191760*b* place the minimum mass of the companion in the brown dwarf regime ( $M \sin i = 38.17 \pm 1.02 M_J$ ). Also the orbital semimajor axis is found to be  $1.35$  AU, well inside the brown dwarf desert region. This so called brown dwarf desert was coined due to the paucity of such objects around solar-like stars with semimajor axes of  $< 3$ – $4$  AU (Marcy & Butler 2000). They showed that fewer than 0.5% of surveyed stars within 3 AU on Doppler programs at the time had brown dwarf companions, whereas 5% of these stars harbour exoplanets. Therefore, since our sample is small (100 stars) we may not statistically expect to detect any brown dwarf desert companions and this object may have an actual mass above the hydrogen burning limit ( $\sim 80 M_J$ ) after inclination effects are considered. For stars with randomly distributed inclinations, 68% are found to fall within  $47^\circ$  (Marcy & Butler 1996a), giving rise to a true mass of  $M = 52.19 M_J$ , comfortably below the hydrogen burning limit. An inclination  $i$  of, or below,  $28.5^\circ$  is required in order for HD191760*b* to be a true stellar companion and such a scenario has an *a priori* probability of only 12.1%. Also there is no binarity flag as of the latest update of the Hipparcos astrometry (van Leeuwen

2007). In addition, a visual inspection of the HARPS spectra does not reveal any evidence for additional stellar lines from an unseen companion and there was no extension of the acquisition image at the telescope to indicate another stellar component, ruling out the possibility of extremely high inclinations. However, such a scenario would agree with the results of Stamatellos & Whitworth (2009) who suggest that brown dwarfs form by disk fragmentation in such systems and that short period radial-velocity companions are preferentially low mass stars. This scenario would agree well with the high orbital eccentricity of the system and could also explain a recent similar discovery from Wittenmyer et al. (2009). Interferometry could be used to help rule out a lower mass stellar companion.

Another way to probe the inclination is to study the rotation velocity along with the activity index from the CaHK lines. The rotation velocity of this star is found to be  $2.33 \pm 0.05$  km/s, using a similar method to that explained in Santos et al. (2002) (the uncertainty is the standard deviation of the 25 measured cross correlation full widths at half maximum), which for the determined radius we find gives an upper limit to the rotation period of 35 days. The estimated rotation period from the  $\log R'_{HK}$ -rotation period correlation (Noyes et al. 1984) is 25.2 days, which is inclination independent and should represent the equatorial rotation period, assuming that the orbital and rotation axes are aligned in the same plane. Assuming the rotation period from the activity relation holds then we estimate the system has a  $\sin i = 0.67$ , which gives an inclination of  $\sim 42^\circ$ . Such an inclination would give rise to an actual mass of  $57 M_J$ , which is still comfortably below the hydrogen burning limit. However, the  $\log R'_{HK}$  activity index was formulated for stars on the main sequence and may be gravity dependent so would not be fully applicable to this star. Also the use of this index should be made only after a number of stellar cycles have been observed, which allows one a robust estimate of the mean  $\log R'_{HK}$ . We have applied the value quoted in Jenkins et al. 2008 (one measurement), not the mean, so we do not know the spread, which can vary at the  $\pm 0.1$  dex level (see Jenkins et al. 2006), and can not apply this to the uncertainty on the relationship itself, which Noyes et al. quote as 0.08 dex for the convective turnover time.

### 6.2 Benchmarkability?

Since HD191760 is found to be evolving off the main sequence onto the sub-giant branch the age estimates for the system can be fairly well constrained. Holmberg et al. (2007) estimate an age of  $5.6^{+0.9}_{-1.9}$  Gyrs in good agreement with our estimated value of  $4.1^{+0.8}_{-2.8}$  Gyrs, the main differences arising due to the differing metallicities, and hence masses, found for this star. The mean of the two estimates gives rise to an age of  $4.9 \pm 1.1$  Gyrs, clearly a fairly old and evolved star. Such an age means that this system could provide a benchmark, evolved system, to test brown dwarf evolutionary models. Given there is a lack of well constrained age estimates for the older population of brown dwarf stars, if one can attain photometry or spectroscopy of the brown dwarf in this system then this could provide a well constrained metallicity and age to use in comparison with current evolutionary models of brown dwarfs (e.g. Baraffe et al. 2003; Burrows et al. 2006). Again interferometry may allow such studies to be

**Table 3.** Radial-velocities for HD48265, HD143361 and HD154672

BJD (-2454000)	RV (m/s)	Uncertainty (m/s)
HD48265		
365.824572	23394.21	3.47
366.874164	23399.40	3.50
367.852214	23395.69	3.45
580.522907	23449.18	3.45
581.553905	23450.06	3.45
724.833698	23413.42	3.45
725.817765	23414.08	3.44
726.779101	23411.87	3.47
HD143361		
250.745318	-437.90	2.39
253.769447	-436.44	3.23
367.556628	-474.74	2.22
368.537299	-474.20	2.24
578.788567	-534.13	2.18
581.807762	-531.75	2.19
HD154672		
248.713853	-3796.59	4.79
250.731312	-3794.42	2.25
367.595129	-3653.29	2.15
368.618599	-3651.00	2.22
578.811238	-3797.81	2.14
581.870548	-3808.85	2.13

performed on this system. Once the inclination is pinned down and the nature of the companion is confirmed as substellar then we can also use the HARPS spectra to obtain a further age constraint from the strength of the lithium line (see Melo et al. 2006). This would provide an additional, and independently determined, age estimate to further constrain the system. In addition, further atomic abundances could be garnered for the star to aid in constraining the metallicity and abundance nature of brown dwarf model atmospheres. Such an abundance study is already underway.

## 7 REFINED ORBITS FOR THE PLANETS AROUND HD48265, HD143361 AND HD154672

Due to some overlap in our target sample with that of the Magellan Planet Search, we can update a few of the recent planet discoveries announced by this program with additional velocities we have found at HARPS. Table 3 shows our absolute Doppler velocities for the three planet host stars HD48265, HD143361 and HD154672. For all of these stars we have acquired observations in three observing runs with overall baselines around one year in duration. Fig. 5 shows the best fits to all three stars using Systemic (Maschiarri et al. 2009), with the Magellan velocities in black (blue) and our HARPS values in grey (green)<sup>1</sup>.

We show the updated orbital solutions in columns 3, 4 and 5 of Table. 4 and in general they agree well with the published results in both Minniti et al. (2009)

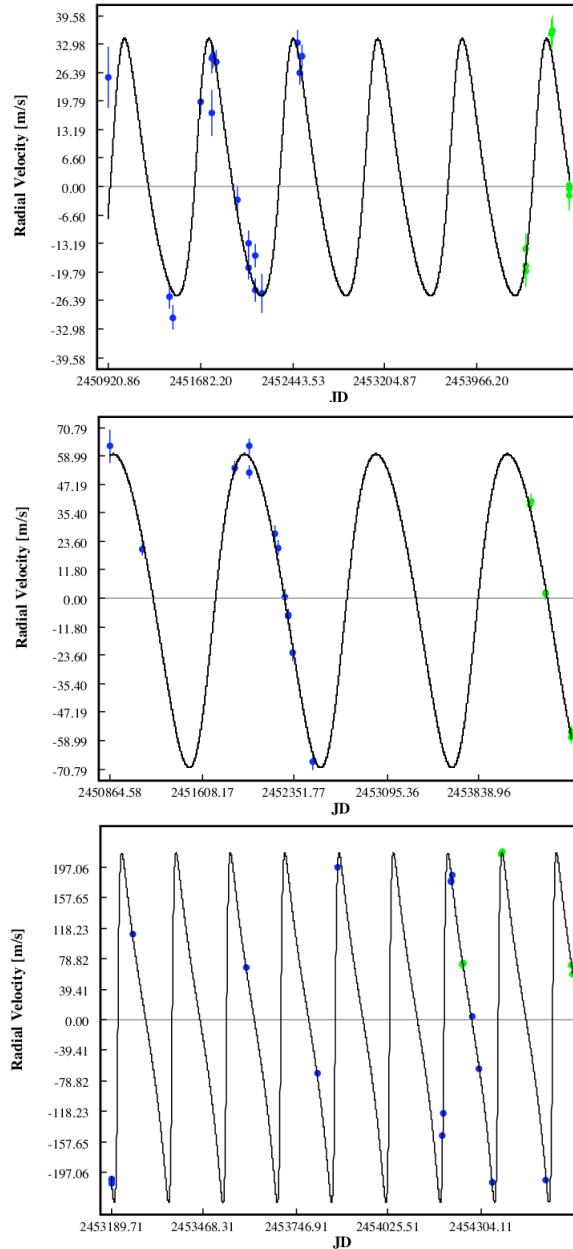


**Figure 5.** The radial-velocity Keplerian fits to the stars HD48265 (top), HD143361 (middle) and HD154672 (bottom). Plotted in blue are the literature values from the Magellan program and in green are the new data points from here.

(HD48265 and HD143361) and López-Morales et al. (2008) (HD154672). López-Morales et al. used 16 velocity points in their orbital solution for HD154672 over a number of orbital periods of the planet. We find a very similar solution with a slightly reduced rms of 3.37 m/s. Note that we used the stellar masses quoted by this group for a direct comparison of the results found.

For HD48265 we find fair agreement with the derived properties assuming a 1-planet Keplerian solution. When adding our eight doppler velocities to the 17 acquired at Magellan, we find that the orbital period is now  $700 \pm 8$  days, albeit with a slightly increased rms of 6.78 m/s. The  $\chi^2_\nu$  also increases when compared to the Magellan data alone from a

<sup>1</sup> Colours in brackets are for the online version of the paper

value of 1.37 up to 3.33. Given the baseline between the two data sets this might argue for an additional companion in the system, however currently both a search in the periodogram of the residuals to the 1-planet fit and the addition of a linear trend do not reveal anything significant. Indeed, although this appears to be the best fit solution, there is no significant power anywhere in the periodogram when combining the two data sets.

Finally, for HD143361*b* we find good agreement with the published results, again with a slightly reduced orbital period of 1057 days and eccentricity of 0.15. This relates to an  $M \sin i$  of 3.12  $M_J$ , in good agreement with the 3  $M_J$  found by Minniti et al. and with a lower rms of 3.37 m/s. For a 1-planet solution none of these three systems exhibit significant trends in the residuals and hence present no evidence, as yet, for additional longer period planets in the system. Note the uncertainties shown in Table. 3 are derived from the updated relation of Wright (2005) (private communication) and the low level of each is highlighted in Fig. 2 where no Ca II H line core emission is seen in any of these three stars (HD48265: top-middle, HD143361: lower-middle and HD154672: bottom).

## 8 SUMMARY

We announce the first four radial-velocity detections from the CHEPS on the ESO-HARPS instrument. The highlight is the discovery of an eccentric brown dwarf in the desert orbiting the metal-rich G3IV-V star HD191760. For the best fit solution, HD191760*b* is found to have a mass of  $38.17 \pm 1.02 M_J$ , an orbital period of  $505.65 \pm 0.42$  days and an eccentricity of  $0.63 \pm 0.01$ , and this discovery adds to the small list of metal-rich stellar-brown dwarf binary systems. Our dynamical simulations show that no additional planets could exist inside the orbit of the brown dwarf with semimajor axes larger than around 0.17 AU due to the destructive tidal forces of the brown dwarf.

Finally, we also confirm the exoplanet detections of HD48265*b*, HD143361*b* and HD154672*b* from the Magellan program by employing 1-planet Keplerian solutions to the data. We show updated orbits by adding eight velocities for HD48265 and six velocities each for HD143361 and HD154672. All orbital parameters are in agreement with the published results by Minniti et al. (2009) and López-Morales et al. (2008). Both HD143361*b* and HD154672*b* show lower rms by the addition of our data, however the best fit for HD48265*b* shows an increased rms and  $\chi^2$ . Since the star is shown to be chromospherically inactive this indicates that additional radial-velocities are required to probe for further companions in this system.

### Acknowledgements

We would like to acknowledge the help from both Ivo Saviane and Oliver Schuetz for observations carried out in the DDT program. J.S.J acknowledges partial support from Centro de Astrofísica FONDAP 15010003, along with partial support from GEMINI-CONICYT FUND and partial support from Comité Mixto ESO-GOBIERNO DE CHILE. K.G. and C.M. are supported by the Polish Ministry of Sciences and Education, Grant No. 1P03D-021-29. We acknowledge the anonymous referee for their helpful comments. We also acknowledge the Simbad and VizieR astronomical

databases. This research has made use of data obtained using the UK's AstroGrid Virtual Observatory Project, which is funded by the Science & Technology Facilities Council and through the EU's Framework 6 programme.

## REFERENCES

- Alibert Y., Mordasini C., Benz W., Winisdoerffer C., 2005, *A&A*, 434, 343
- Alonso A., Arribas S., Martinez-Roger C., 1996, *A&A*, 313, 873
- Anglada-Escude G., Lopez-Morales M., Chambers J. E., 2008, ArXiv e-prints
- Baraffe I., Chabrier G., Barman T. S., Allard F., Hauschildt P. H., 2003, *A&A*, 402, 701
- Blackwell D. E., Petford A. D., Arribas S., Haddock D. J., Selby M. J., 1990, *A&A*, 232, 396
- Burrows A., Sudarsky D., Hubeny I., 2006, *ApJ*, 640, 1063
- Demarque P., Woo J.-H., Kim Y.-C., Yi S. K., 2004, *ApJS*, 155, 667
- Edvardsson B., Andersen J., Gustafsson B., Lambert D. L., Nissen P. E., Tomkin J., 1993, *A&A*, 275, 101
- Fischer D. A., Valenti J., 2005, *ApJ*, 622, 1102
- Girardi L., Bressan A., Bertelli G., Chiosi C., 2000, *A&AS*, 141, 371
- Gonzalez G., 1997, *MNRAS*, 285, 403
- Goździewski K., Konacki M., 2006, *ApJ*, 647, 573
- Goździewski K., Konacki M., Maciejewski A. J., 2003, *ApJ*, 594, 1019
- Henry G. W., Donahue R. A., Baliunas S. L., 2002, *ApJL*, 577, L111
- Holmberg J., Nordström B., Andersen J., 2007, *A&A*, 475, 519
- Holmberg J., Nordström B., Andersen J., 2008, ArXiv e-prints
- Houk N., 1978, Michigan catalogue of two-dimensional spectral types for the HD stars. Ann Arbor : Dept. of Astronomy, University of Michigan : distributed by University Microfilms International, 1978-
- Jenkins J. S., Jones H. R. A., Pavlenko Y., Pinfield D. J., Barnes J. R., Lyubchik Y., 2008, *A&A*, 485, 571
- Jenkins J. S., Jones H. R. A., Tinney C. G., Butler R. P., McCarthy C., Marcy G. W., Pinfield D. J., Carter B. D., Penny A. J., 2006, *MNRAS*, 372, 163
- Kaufer A., Stahl O., Tubbesing S., Norregaard P., Avila G., Francois P., Pasquini L., Pizzella A., 1999, *The Messenger*, 95, 8
- Kornet K., Bodenheimer P., Różycka M., Stepinski T. F., 2005, *A&A*, 430, 1133
- Kurucz R., 1993, ATLAS9 Stellar Atmosphere Programs and 2 km/s grid. Kurucz CD-ROM No. 13. Cambridge, Mass.: Smithsonian Astrophysical Observatory, 1993., 13
- Lin D. N. C., Papaloizou J., 1986, *ApJ*, 309, 846
- López-Morales M., Butler R. P., Fischer D. A., Minniti D., Shectman S. A., Takeda G., Adams F. C., Wright J. T., Arriagada P., 2008, *AJ*, 136, 1901
- Marcy G. W., Butler R. P., 1996a, *ApJL*, 464, L147+
- Marcy G. W., Butler R. P., 1996b, in *Proc. SPIE Vol. 2704*, p. 46-49, The Search for Extraterrestrial Intelligence (SETI) in the Optical Spectrum II, Stuart A. Kingsley;

**Table 4.** Orbital parameters for HD191760*b*, HD48265*b*, HD143361*b* and HD154672*b*.

Parameter	HD191760 <i>b</i>	HD48265 <i>b</i>	HD143361 <i>b</i>	HD154672 <i>b</i>
Orbital period $P$ (days)	505.65±0.42	700±8	1057±20	163.9±0.1
Velocity amplitude $K$ (m/s)	1047.83±38.71	28.3±9.0	65.1±26.3	226.52±9.22
Eccentricity $e$	0.63±0.01	0.18±0.13	0.15±0.17	0.61±0.02
$\omega$ (°)	200.37±0.28	309±27	237±55	266±2
$T_0$ (JD-2,450,000)	4835.65±2.06	4486±50	3746±147	4520±1
$M \sin i$ ( $M_J$ )	38.17±1.02	1.16±0.38	3.12±1.44	5.02±0.17
Semimajor axis $a$ (AU)	1.35	1.51	2.00	0.60
rms (m/s)	2.00	6.756	3.37	3.37
$\chi^2_\nu$	1.04	3.33	2.42	2.14
$N_{\text{Obs}}$	29	25*	18	22

- Guillermo A. Lemarchand; Eds. First three planets. pp 46–49
- 3529
- Wright J. T., 2005, *PASP*, 117, 657
- Marcy G. W., Butler R. P., 2000, *PASP*, 112, 137
- Maschiari S., Rivera E., Wolf S., Laughlin G., 2009, in prep
- Mayor M., Pepe F., Queloz D. e. a., 2003, *The Messenger*, 114, 20
- Mayor M., Queloz D., 1995, *Nature*, 378, 355
- Melo C., Santos N. C., Pont F., Guillot T., Israelian G., Mayor M., Queloz D., Udry S., 2006, *A&A*, 460, 251
- Michtchenko T. A., Ferraz-Mello S., 2001, *AJ*, 122, 474
- Migaszewski C., Nowak G., 2009, ArXiv e-prints
- Minniti D., Butler R. P., López-Morales M., Shectman S. A., Adams F. C., Arriagada P., Boss A. P., Chambers J. E., 2009, *ApJ*, 693, 1424
- Nordström B., Mayor M., Andersen J., Holmberg J., Pont F., Jørgensen B. R., Olsen E. H., Udry S., Mowlavi N., 2004, *A&A*, 418, 989
- Noyes R. W., Hartmann L. W., Baliunas S. L., Duncan D. K., Vaughan A. H., 1984, *ApJ*, 279, 763
- O’Toole S. J., Tinney C. G., Jones H. R. A., 2008, *MNRAS*, 386, 516
- Pagel B. E. J., Tautvaisiene G., 1995, *MNRAS*, 276, 505
- Pavlenko Y. V., 2000, *Astronomy Reports*, 44, 219
- Pepe F., Mayor M., Queloz D., Benz W., Bonfils X., Bouchy F., Curto G. L., Lovis C., Mégevand D., Moutou C., Naef D., Rupprecht G., Santos N. C., Sivan J.-P., Sosnowska D., Udry S., 2004, *A&A*, 423, 385
- Perryman M. A. C., Lindegren L., Kovalevsky e. a., 1997, *A&A*, 323, L49
- Pinsonneault M. H., DePoy D. L., Coffee M., 2001, *ApJL*, 556, L59
- Queloz D., Henry G. W., Sivan J. P., Baliunas S. L., Beuzit J. L., Donahue R. A., Mayor M., Naef D., Perrier C., Udry S., 2001, *A&A*, 379, 279
- Saar S. H., Butler R. P., Marcy G. W., 1998, *ApJL*, 498, L153
- Saar S. H., Donahue R. A., 1997, *ApJ*, 485, 319
- Santos N. C., Mayor M., Naef D., Pepe F., Queloz D., Udry S., Blecha A., 2000, *A&A*, 361, 265
- Santos N. C., Mayor M., Naef D., Pepe F., Queloz D., Udry S., Burnet M., Clausen J. V., Helt B. E., Olsen E. H., Pritchard J. D., 2002, *A&A*, 392, 215
- Stamatellos D., Whitworth A. P., 2009, *MNRAS*, 392, 413
- Trilling D. E., Lunine J. I., Benz W., 2002, *A&A*, 394, 241
- van Leeuwen F., 2007, *A&A*, 474, 653
- Wittenmyer R. A., Endl M., Cochran W. D., Ramírez I., Reffert S., MacQueen P. J., Shetrone M., 2009, *AJ*, 137,